Effects of Catalyst Layer and Gas Diffusion Layer Thickness on the Performance of Activated Carbon Air-cathode for Microbial Fuel Cells

Xiaojing Li[1,2], Xin Wang[1,*], Yueyong Zhang[1], Ningshengjie Gao[1], Desheng Li[2], Qixing Zhou[1,*]

[1] MOE Key Laboratory of Pollution Processes and Environmental Criteria / Tianjin Key Laboratory of Environmental Remediation and Pollution Control / College of Environmental Science and Engineering, Nankai University, Tianjin 300071, China
[2] School of Environmental Science and Safety Engineering, Tianjin University of Technology, Tianjin 300384, China
[*]E-mail: zhouqx@nankai.edu.cn; xinwang1@nankai.edu.cn

There are three key species to transport in AC air-cathodes, including O_2, H_2O and OH^-. The thickness of GDL could be an apparent and easy-controlled parameter to optimize the O_2 transport while the thickness of CLs is important to the transport of not only O_2 but also H_2O and OH^-. In terms of maximum power density, the optimal thickness of CL was 0.2 mm with the highest power density of 2348 ± 80 mW·m^{-2} obtained using 0.3 mm of GDL. According to the correlation analysis, the thickness of CL (Pearson correlation coefficient of 0.709) played a more important role than that of GDL (Pearson correlation coefficient of 0.542) on the exchange current density and the maximum power density. The thickness of GDL was mainly related to the charge transfer resistance which accounted for 49–87% of the total internal resistance. The correlation analysis also showed that the total thickness of air-cathode had a significant correlation to the exchange current density. The thickness of CL was more significant than GDL on the exchange current density and maximum power density with the optimal thickness of 0.2 mm. The thickness of GDL was mainly related to the charge transfer resistance.

1. INTRODUCTION

Microbial fuel cell (MFC) is a promising system where microorganisms acted as catalysts to convert chemical energy into electrical energy [1, 2]. The primary benefit of the MFC from the view

point of energy is to reduce the energy needed through the decrease of both energy consumption and the production of secondary sludge [3]. To improve the power output of MFCs for the future application, the performance of the cathode has been considered as one of the largest bottlenecks which need to be improved [4].

The air-cathode is one of the most widely-used cathodes with one side directly exposed to the air. It is usually consisted of a gas diffusion layer (GDL), a current collector and a catalyst layer (CL). Polytetrafluoroethene (PTFE) was usually used in the GDL to avoid leaking and transfer oxygen. Metal meshes are the most widely used as the current collector, such as stainless steel mesh due to its low cost and anticorrosion [5, 6]. The CL is studied intensively from compound substances [7, 8] to elementary [9], from metals [10] to nonmetal materials [11]. However, the air-cathode is not economically applicable until the expensive catalyst made of precious metals was substituted by low-cost materials such as activated carbon (AC) [12, 13].

Compared to the method of brushing, the rolling-press has advantages of good reproducibility, simple operation and labor-saving [14]. There are three key species to transport in AC air-cathodes, including O_2, H_2O and OH^-. The thickness of GDL could be an apparent and easy-controlled parameter to optimize the O_2 transport. Similarly, the thickness of CLs is important to the transport of not only O_2 but also H_2O and OH^-.

In order to investigate the effect of GDL or CL thickness on the cathodic performance, GDLs and CLs with different thickness were assembled to nine AC air-cathodes. The performances were tested in terms of power output, current density and internal resistance.

2. MATERIALS AND METHODS

2.1 Fabrication of Air-cathodes

All cathodes consisted of a stainless steel mesh (40×40 mesh, type 304, Detiannuo Commercial Trade Co. Ltd., Tianjin, China) with a CL rolled on the water facing side and a GDL rolled on the air facing side. Cathodes were made by rolling-press method according to previous description [14, 15] with a slight change. Firstly, the time of ultrasonic agitation before and after dripping PTFE emulsion (60 wt%, Hesen, Shanghai, China) was reduced to 10 min to avoid destroying the fine mixture of PTFE and carbon. Secondly, water or ethanol was not used during the rolling-press process in order to make the bond the GDL and CL to the stainless steel mesh stronger. The GDL was made of carbon black (Jinqiushi Chemical Co. Ltd., Tianjin, China) and PTFE emulsion with a mass ratio of 3:7. The GDL film was rolled on a stainless steel mesh and followed by heating at 340 °C for 20 min [6]. The CL was made of activated carbon (Xinsen Carbon Co. Ltd., Fujian, China) and PTFE emulsion with a mass ratio of 6:1. AC air-cathodes were dried at room temperature for at least 24 h before installed in MFCs.

AC air-cathodes with different thickness of CL and GDL were prepared and marked as *xGyC*, where *x* (mm) is the thickness of GDL and *y* (mm) is the thickness of CL. The nine different AC air-

cathodes were marked as: 0.3G0.1C, 0.3G0.2C, 0.3G0.3C, 0.5G0.1C, 0.5G0.2C, 0.5G0.3C, 0.7G0.1C, 0.7G0.2C, 0.7G0.3C.

2.2 MFC Construction and Operation

MFCs were single chambered cubic-shaped reactors as described previously (4 cm long and 3 cm in diameter) [9]. All anodes were carbon fiber brushes soaked overnight by acetone [16]. MFCs were inoculated with the effluent from three MFCs operated for over one year. The medium contained a phosphate buffer nutrient solution (50 mM PBS; $Na_2HPO_4 \cdot 12H_2O$ 10.317 $g \cdot L^{-1}$; $NaH_2PHO_4 \cdot 2H_2O$ 3.321 $g \cdot L^{-1}$; NH_4Cl 0.31 $g \cdot L^{-1}$; KCl 0.13 $g \cdot L^{-1}$), a trace mineral solution (12.5 $mL \cdot L^{-1}$), a vitamin solution (5 $mL \cdot L^{-1}$) and sodium acetate (1.0 $g \cdot L^{-1}$) [17]. All reactors were refilled each time when the voltage decreased to less than 50 mV, forming a complete cycle at 30 °C in constant temperature incubator.

2.3 Calculations and Measurements

Polarization and power density curves were measured by varying the external resistance from 1000 to 30 Ω with a time interval of 25 min to ensure a stable voltage at the 3rd cycle of MFCs where the anodes were well pre-acclimated. Coulombic efficiencies (CEs) were calculated as CE = C_h/C_t, where C_h is the amount of Coulombs harvested in one cycle and C_t is the theoretical Coulombs calculated from the complete oxidation of acetate as $C_t = F\ b\ M\ v$. F is Faraday's constant (96485 $C \cdot mol\text{-}e^{-1}$), b is the number of electrons produced per mol of substrate (8 mol-e mol-acetate^{-1}), M is the acetate concentration and v is the liquid volume (28 mL).

The linear fit and the non-linear surface fit were performed using Origin 9.0. Non-linear surface fit equation were calculated as $z = c_0 + c_1x + c_2y + c_{12}xy + c_{11}x^2 + c_{22}y^2$, where x (mm) is thickness of GDL, y (mm) is thickness of CL, z_1 ($mW \cdot m^{-2}$) is maximum power density, z_2 ($A \cdot m^{-2}$) is exchange current density, z_3 (Ω) is current transfer resistance and c_0, c_1, c_2, c_{12}, c_{11}, c_{22} are the corresponding constant coefficients. The Pearson correlation coefficient at 0.01/0.05 level (significant 2-tail test, n = 9) was obtained by using Bivariate Analysis of Statistical Product and Service Solutions 19.0.

2.4 Electrochemical Analysis

Before electrochemical tests, cathodes were soaked in 50 mM PBS in abiotic reactors for at least 24 h. The target cathode was used as the working electrode, a platinum sheet of 1 cm^2 was used as the counter electrode and a saturated calomel electrode (3 M KCl, 0.241 V versus standard hydrogen electrode) was used as the reference electrode. All the electrochemical tests were performed in the same reactor using a firmly fixed reference electrode and refilling the same PBS electrolyte.

Linear sweep voltammetry (LSV) was conducted from 0.3 to −0.2 V at the scan rate of 0.1 $mV \cdot s^{-1}$. Tafel plots (log |current density|, $A \cdot m^{-2}$, versus |overpotential|, V) were recorded by sweeping

the overpotential ($|\eta|$, mV) from 0 to 100 mV at the scan rate of 0.1 mV·s^{-1}, where $\eta = 0$ is the open circuit potential (OCP).

Electrochemical impedance spectrum (EIS) was performed over a frequency range from 100 kHz to 10 mHz with a sinusoidal perturbation signal amplitude of 10 mV using a potentiostat (Autolab PGSTAT 302N, Metrohm, Switzerland) at OCP. The Nyquist plots were used to interpret the spectra. A fitting program (ZsimpWin 3.10) was employed to simulate plots according to an equivalent circuit reported previously [6].
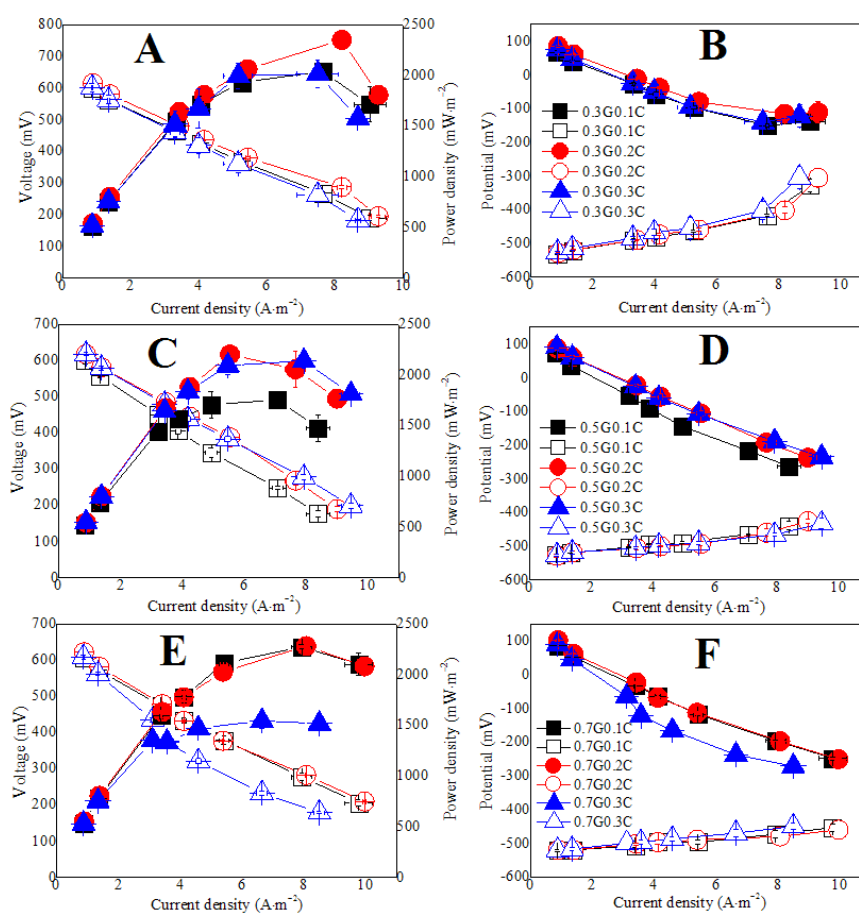
3. RESULTS

3.1 Performance of MFCs

Figure 1. Polarization curves and power density curves (A/C/E) and electrode potentials (B/D/F) of MFCs using different air-cathodes. A and B: 0.3G*y*C, C and D: 0.5G*y*C, E and F: 0.7G*y*C.

No matter the thickness of GDL was 0.3, 0.5 or 0.7 mm, the highest power densities of 2348±80, 2201±24, 2280±11 mW·m^{-2} were achieved in those cathodes with the CL thickness of 0.2 mm respectively (*x*G0.2C, Figure 1A, C and E, Table S1). The lowest power density of 1543±78 mW·m^{-2} was observed in the MFC with 0.7G0.3C cathode, which had the thickest GDL (0.7 mm) and

CL (0.3 mm) (Figure 1E, Table S1). The cathodic potentials at their highest power densities tend to decrease with the increase of GDL thickness. For example, the cathodic potential decreased from −141 to −189 mV and −237 mV when the thickness of GDL increased from 0.3 to 0.5 mm and to 0.7 mm with the same 0.3 mm of CL.

The *x*G0.2C cathodes exhibited the highest open circuit voltages (OCVs) of 661±4, 652±12 and 655±4 mV and the highest OCPs of 246, 228 and 230 mV with 0.3, 0.5 and 0.7 mm of GDLs respectively (Figure S1), which was consistent with the power density results.

CEs at the start-up period, stationary period and non-equilibrium period were showed in supporting information (Figure S2). In the first period (from the 1st to 3rd cycle, or from 0 to 200 h), MFCs using 0.2 mm of CL exhibited a faster voltage increase than other MFCs with the same GDL thickness (Figure S2A, B and C). When CE reached to ~25% (the 4th cycle), the inoculation was stopped and a relative stable CEs were obtained from the 4th to 7th cycle (from 200 to 350 h). From the 8th cycle, the inoculation was restarted, resulted in a further increase in CEs with a non-stable trend, indicating that the inoculation played an important role in CEs.
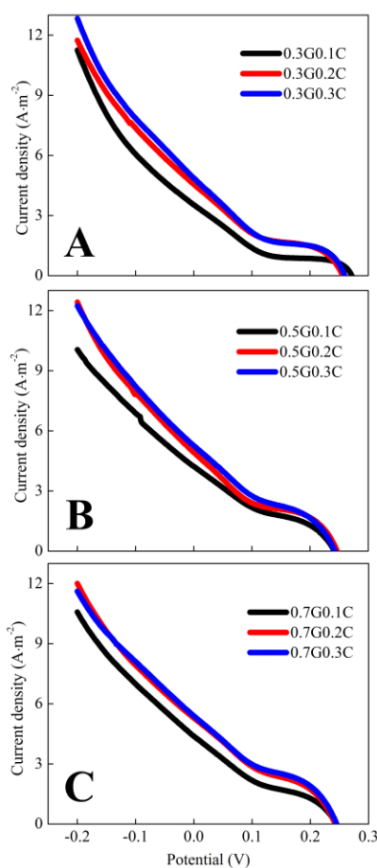
3.2 LSVs and Tafel Plots of Air-cathodes

Figure 2. Abiotic LSVs of different air-cathodes in 50 mM PBS (pH = 7) at room temperature. A saturated calomel electrode was used as the reference electrode.

With the same thickness of GDL, current densities increased with the thickness of CL over the potential range from –0.1 to 0.2 V (Figure 2). For example, at the potential of 0 V (versus saturated calomel electrode), current densities of 4.23, 4.93 and 5.26 A·m^{-2} were achieved in 0.5G0.1C, 0.5G0.2C and 0.5G0.3C air-cathodes respectively (Figure 2B). Although the current densities also increased with the thickness of GDLs, the influence was not as obvious as that of CLs.

According to Tafel plots and linear fitting results at potentials from 80 to 100 mV, the exchange current densities (j_0, A·m^{-2}) increased with the thickness of CL or GDL (Figure S3, Table S2). The highest exchange current density of 1.89 A·m^{-2} was achieved by the 0.7G0.3C, which was inconsistent with the result of power densities.

3.3 EIS of MFCs

Despite of the similar ohmic resistance (R_s), the charge transfer resistance (R_{ct}) was the dominant part of the total internal resistance (R_{in}) accounting for a proportion of 49–87% (Figure 3 and Figure S4). The R_{ct} tend to be decreased with the increase of CL thickness except the 0.7G0.3C using the thickest GDL and CL.
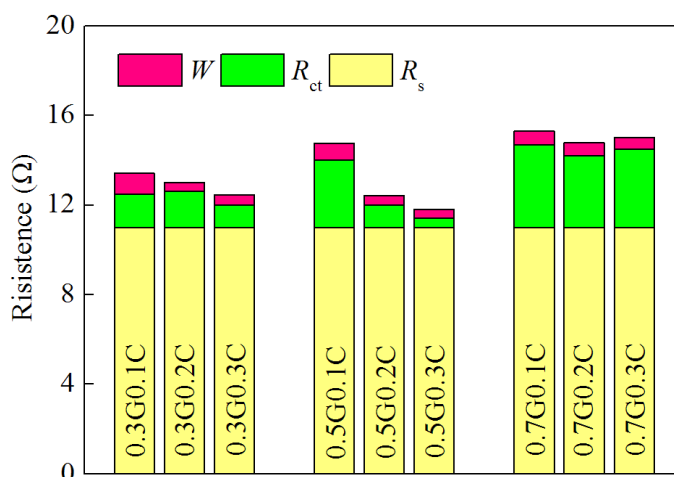

Figure 3. Resistances analysis of different air-cathodes at OCP based on EIS.

With the same thickness of GDL, the double layer capacitances (C_{dl}) of xG0.2C were larger than those of xG0.1C and xG0.3C (Table S3). No obvious trend was observed between the thickness of GDL and the C_{dl}. The changes of Warburg diffusion impedance (W) in different cathodes were insignificant compared to R_{ct} and C_{dl}.

4. DISCUSSION

The maximum power densities were affected by the thickness of both CL and GDL. With the same thickness of GDL, the highest power densities were achieved with the optimal CLs of 0.2 mm,

which was consistent with the results that the thickness of the CL had an optimal value [18, 19]. However, different from power densities, the exchange current density increased with the thickness of both GDL and CL, possibly due to the absent of biofilm in LSV tests. This result indicated that a dynamic test such as LSVs could not be transferable to the real performance in MFCs [20].

The xG0.2C cathodes exhibited large C_{dl} and high power densities, suggesting that the high power output may be partly from the large capacitance in double layer, because the capacitance could sustain a high current densities under the same cathodic potential by the transient storage of excess charge [6]. The R_{ct} accounted for 49–87% of R_{in} and thus significantly affected the power output. Therefore, to reduce the R_{ct} was a feasible approach to improve the performance of MFCs in the future.

Table 1. Pearson correlation coefficient (significant 2-tail test), n = 9

Index	GDL	CL	MPD	j_0	R_{ct}	C_{dl}
GDL	1					
CL	0.000 (1.000)	1				
MPD	−0.164 (0.673)	−0.200 (0.607)	1			
j_0	0.542 (0.132)	0.709[*] (0.032)	−0.156 (0.689)	1		
R_{ct}	0.729[*] (0.026)	−0.382 (0.311)	−0.296 (0.440)	0.074 (0.851)	1	
C_{dl}	0.549 (0.126)	−0.085 (0.828)	0.433 (0.244)	0.354 (0.350)	0.546 (0.129)	1

[*]: significant correlation at P < 0.05 (2-tail).

Table 2. Non-linear surface fit parameter for MPD, CL and GDL (n = 9, R = 0.9991).

variable	DF	parameter estimates	standard error	t value	Pr> | t |	Standardized estimate
Intercept		1865.11111	49.75098	37.49	< 0.0001	0
c_1	1	-2534.16667	170.14677	-14.89	0.0007	-2.38238
c_2	1	9515.41667	287.11787	33.14	< 0.0001	4.47273
c_{12}	1	3962.50000	230.12426	17.22	0.0004	1.23081
c_{11}	1	1408.33333	162.72243	8.65	0.0032	1.33277
c_{22}	1	-25866.66667	650.88970	-39.74	< 0.0001	-4.91386

c_1: GDL, c_2: CL, c_{12}: reciprocal action (GDL and CL), c_{11}: reciprocal action (GDL and GDL), c_{22}: reciprocal action (CL and CL), similarly hereinafter.

The optimal assembly was 0.3G0.2C in terms of MPD. The CL played a more important role for air-cathodes than the GDL according to apparent variation degree of MPDs and j_0. The Pearson correlation coefficient of –0.200 between MPD and the thickness of CL was slightly higher than −0.164 between MPD and GDL (Table 1), which was also demonstrated by the non-linear surface fitting involving the reciprocal action (standardized estimate 4.47273 > 2.38238, Table 2, Figure 4A). Furthermore, the Pearson correlation coefficient (0.709) between the thickness of CL and j_0 achieved a

statistically significant level (P < 0.05) compared to 0.542 between the thickness of GDL and j_0, indicating that the thickness of CL was mainly responsible to the differences in exchange current density, which was consistent with the non-linear surface fitting (3.03726 > 2.39885, Table S4, Figure 4B). The correlation between j_0 and the total thickness (GDL + CL) in Figure S5 showed a significant correlation (R = 0.72163, P < 0.05, n = 9), indicating that the total thickness of air-cathode exerted a vital effect on j_0.
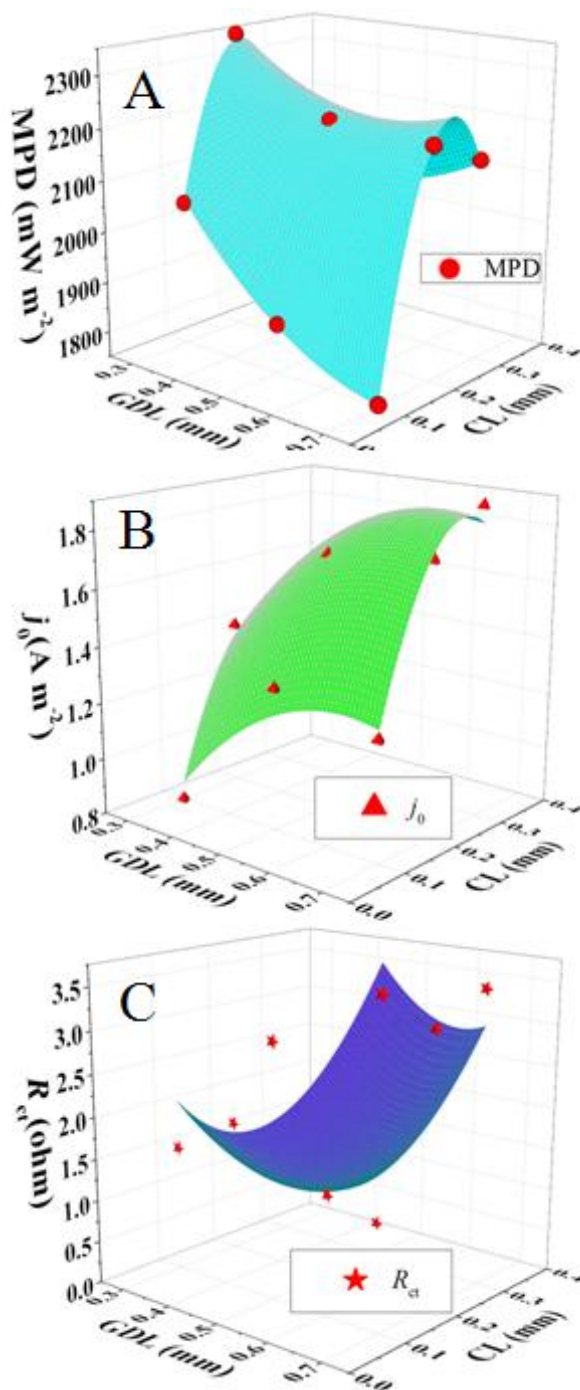
Figure 4. Non-linear surface fitting graph of maximum power density (MPD) and thickness of CL and GDL (A), exchange current density (j_0) and thickness of CL and GDL (B) and charge transfer resistance and thickness of CL and GDL (C).

The R_{ct} positively correlated with the thickness of GDL (P < 0.05) as proved by the non-linear surface fitting (2.67164 > 1.20571, Table S5, Figure 4C), showing the GDL played an important role in R_{ct}. The reason for the influence on R_{ct} by the GDL needs to be investigated in the future. The highest Pearson correlation coefficient (only 0.433, P < 0.05, Table 1) was observed between the MPD and C_{dl}, suggesting that the MPD was also determined by other factors such as the cathodic microbial community.

5. CONCLUSION

The thickness of CL played a more important role than that of GDL on both the maximum power density in biotic tests and the exchange current density in abiotic measurements according to the correlation analysis. However, the thickness of GDL had a more significant effect on the charge transfer resistance. These results provided more information on the optimization of CL and GDL in AC air-cathodes in the future.

References

1. B. E. Logan, *Microbial fuel cells*, Wiley-Interscience, New York (2008).
2. K. Rabaey, L. Angenent, U. Schröder and J. Keller, *Bio-electrochemical Systems: From Extracellular Electron Transfer to Biotechnological Application*, IWA publishing, London (2010).
3. Z. He, *Environmental science & technology*, 47 (2012) 332.
4. B. E. Logan, *Applied microbiology and biotechnology*, 85 (2010) 1665.
5. F. Zhang, T. Saito, S. A. Cheng, M. A. Hickner and B. E. Logan, *Environmental science & technology*, 44 (2010) 1490.
6. X. J. Li, X. Wang, Y. Y. Zhang, N. Ding and Q. X. Zhou, *Applied Energy*, 123 (2014) 13.
7. F. Zhao, F. Harnisch, U. Schröder, F. Scholz, P. Bogdanoff and I. Herrmann, *Electrochemistry Communications*, 7 (2005) 1405.
8. E. H. Yu, S. A. Cheng, K. Scott and B. Logan, *Journal of Power Sources*, 171 (2007) 275.
9. X. Wang, Y. J. Feng, H. M. Wang, Y. P. Qu, Y. L. Yu, N. Q. Ren, N. Li, E. Wang, H. Lee and B. E. Logan, *Environmental science & technology*, 43 (2009) 6088.
10. S. A. Cheng, H. Liu and B. E. Logan, *Environmental science & technology*, 40 (2006) 364.
11. W. Z. Li, C. H. Liang, W. J. Zhou, J. S. Qiu, Z. Zhou, G. Q. Sun and Q. Xin, *The Journal of Physical Chemistry B*, 107 (2003) 6292.
12. F. Zhang, S. A. Cheng, D. Pant, G. V. Bogaert and B. E. Logan, *Electrochemistry Communications*, 11 (2009) 2177.

13. H. Dong, H. B. Yu and X. Wang, *Environmental science & technology*, 46 (2012) 13009.
14. H. Dong, H. B. Yu, X. Wang, Q. X. Zhou and J. L. Feng, *Water Research*, 46 (2012) 5777.
15. H. Dong, H. B. Yu, H. Yu, N. S. J. Gao and X. Wang, *Journal of Power Sources*, 232 (2013) 132.
16. X. Wang, S. A. Cheng, Y. J. Feng, M. D. Merrill, T. Saito and B. E. Logan, *Environmental science & technology*, 43 (2009) 6870.
17. D. R. Lovley and E. J. Phillips, *Applied and environmental microbiology*, 54 (1988) 1472.
18. X. Y. Zhang, J. Shi, P. Liang, J. C. Wei, X. Huang, C. Y. Zhang and B. E. Logan, *Bioresource technology*, 142 (2013) 109.
19. B. Wei, J. C. Tokash, G. Chen, M. A. Hickner and B. E. Logan, *RSC Advances*, 2 (2012) 12751.
20. T. Saito, T. H. Roberts, T. E. Long, B. E. Logan and M. A. Hickner, *Energy & Environmental Science*, 4 (2011) 928.

Supporting Information:

Table S1 Maximum power density of MFCs using different AC air-cathodes, unit: $mW \cdot m^{-2}$.

GDL(mm)	CL(mm)		
	0.1	0.2	0.3
0.3	2037±26	2348±80	2013±133
0.5	1753±78	2201±24	2138±77
0.7	2272±23	2280±11	1543±78

Table S2 Linear fit equations and exchange current densities calculated from the linear region of the Tafel plots.

Air-cathodes		Fit linear equation	R^2	j_0 ($A \cdot m^{-2}$)
0.3G	0.1C	y = 0.40021x - 0.0951	0.96414	0.80
	0.2C	y = 0.79962x + 0.14236	0.97058	1.39
	0.3C	y = 0.57045x + 0.14978	0.91662	1.41
0.5G	0.1C	y = 1.4408x + 0.11271	0.99392	1.30
	0.2C	y = 0.88315x + 0.23322	0.97178	1.71
	0.3C	y = 1.40708x + 0.22173	0.99166	1.67
0.7G	0.1C	y = 1.56813x + 0.08627	0.99341	1.22
	0.2C	y = 1.37044x + 0.2419	0.99323	1.75
	0.3C	y = 1.31089x + 0.2759	0.99378	1.89

Table S3 R_s, R_{ct}, W and capacitance of different air-cathodes at their OCPs.

elememt	0.3G			0.5G			0.7G		
	0.1C	0.2C	0.3C	0.1C	0.2C	0.3C	0.1C	0.2C	0.3C
$R_s(\Omega)$	11	11	11	11	11	11	11	11	11
$R_{ct}(\Omega)$	1.5	1.6	1.0	3.0	1.0	0.4	3.7	3.2	3.5
$W(\Omega \cdot s^{1/2})$	0.9	0.4	0.5	0.8	0.4	0.4	0.6	0.6	0.5
$C_{dl}(\Omega^{-1} \cdot s^n)$	2.8×10^{-5}	8.7×10^{-4}	1.8×10^{-5}	2.4×10^{-5}	5.1×10^{-4}	5.8×10^{-5}	8.9×10^{-4}	1.0×10^{-3}	6.2×10^{-4}
n	0.9	0.7	1	0.7	0.6	0.8	0.7	0.7	0.8

Table S4 Non-linear surface fit parameters for j_0, CL and GDL (n = 9, R = 0.9699)

Variable	DF	Parameter estimates	Standard error	t value	Pr > |t|	Standardized estimate
Intercept	1	-1.16083	0.51369	-2.26	0.1089	**0**
c_1	1	4.65000	1.75681	2.65	0.0772	**2.39885**
c_2	1	11.77500	2.96457	3.97	0.0285	**3.03726**
c_{12}	1	0.75000	2.37610	0.32	0.7730	**0.12784**
c_{11}	1	-3.75000	1.68015	-2.23	0.1118	**-1.94741**
c_{22}	1	-23.50000	6.72062	-3.50	0.0396	**-2.44977**

Table S5 Non-linear surface fit parameters for R_{ct}, CL and GDL (n = 9, R = 0.8333)

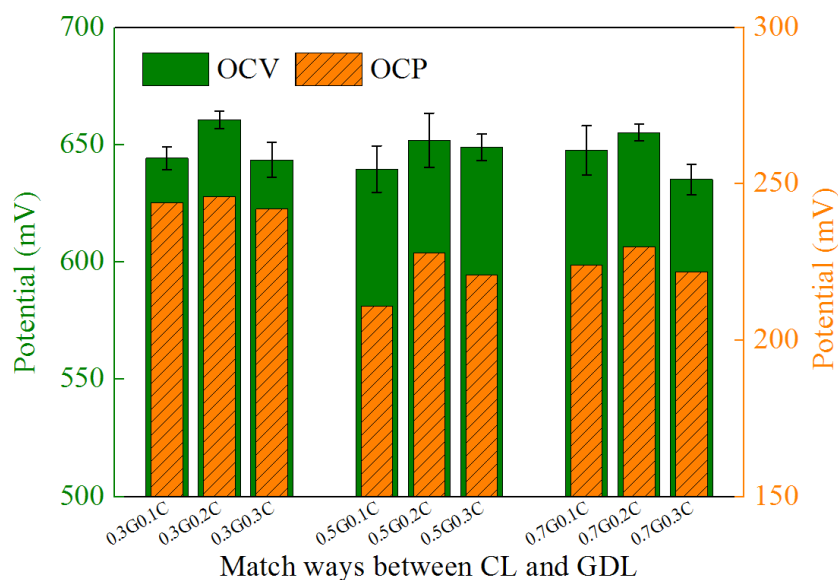| Variable	DF	Parameter estimates	Standard error	t value	Pr > |t|	Standardized estimate
Intercept	1	7.0875	4.49769	1.58	0.2132	**0**
c_1	1	-19.2500	15.38194	-1.25	0.2995	**-2.67164**
c_2	1	-17.3750	25.95659	-0.67	0.5512	**-1.20571**
c_{12}	1	3.7500	20.80415	0.18	0.8684	**0.17196**
c_{11}	1	23.7500	14.71075	1.61	0.2048	**3.31808**
c_{22}	1	25.0000	58.84301	0.42	0.6996	**0.70112**

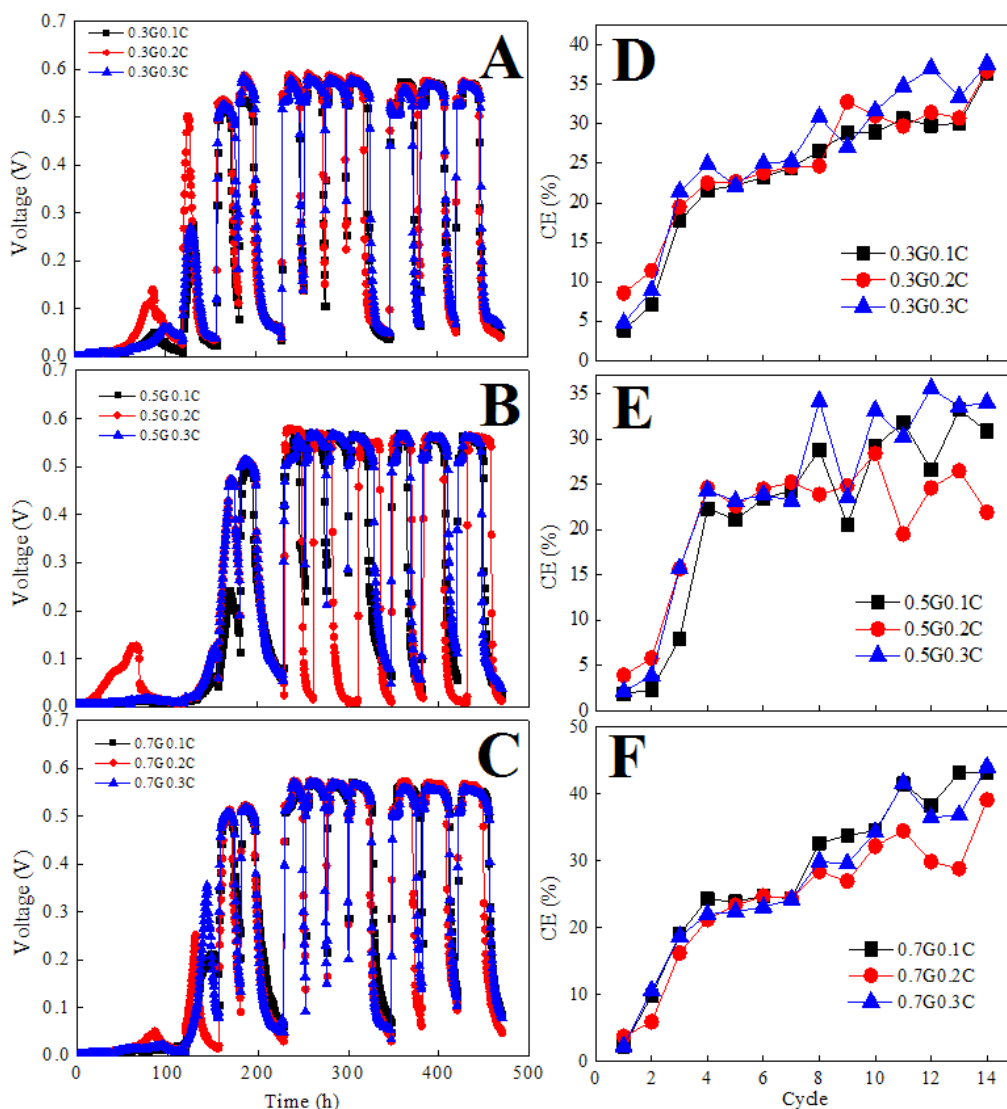Figure S1 Open circuit voltages and open circuit potentials of MFCs using different AC air-cathodes.

Figure S2 Voltage curves (A/B/C) and CEs (D/E/F) of MFCs using different AC air-cathodes. A and D: 0.3G*y*C, B and E: 0.5G*y*C, C and F: 0.7G*y*C.
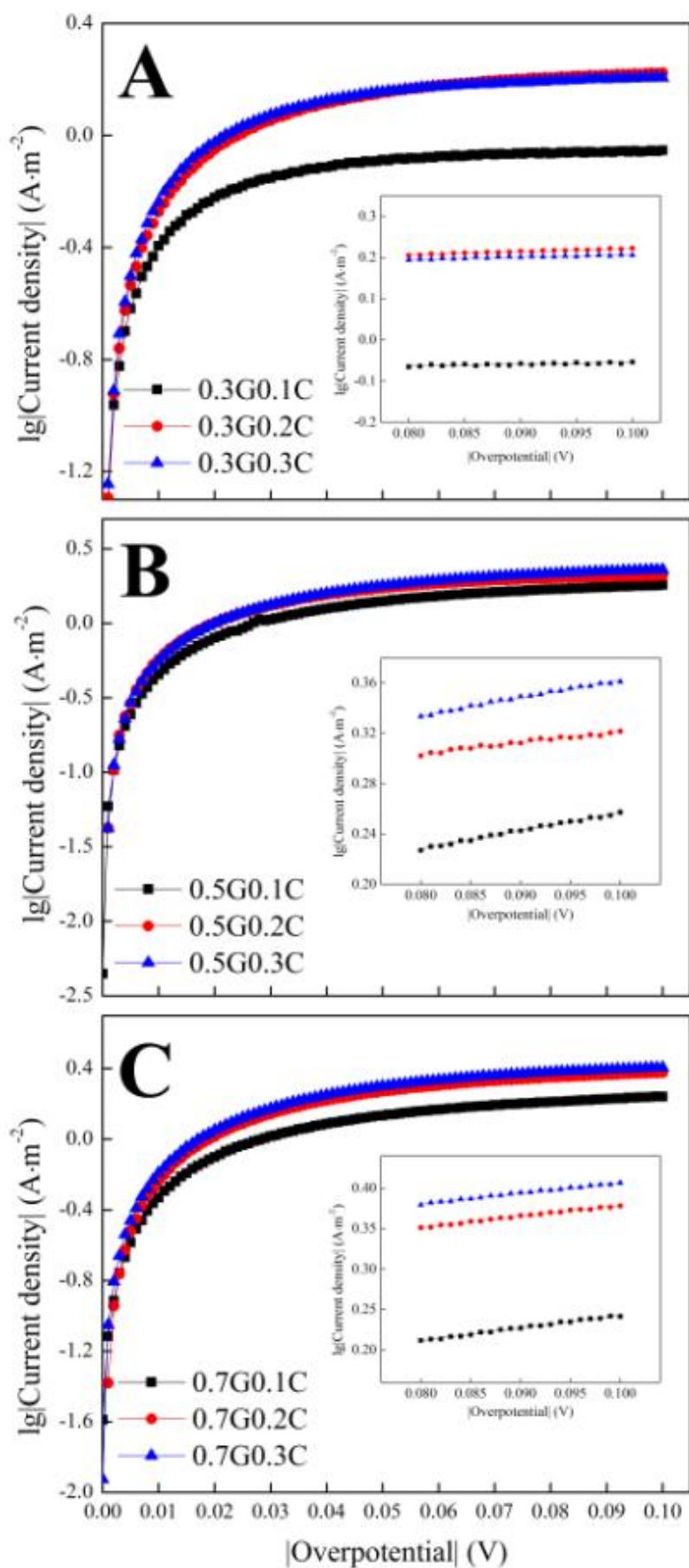
Figure S3 Tafel plots of different AC air-cathodes. The inserted figure is the linear fitting for the Tafel plots at overpotentials from 80 to 100 mV.
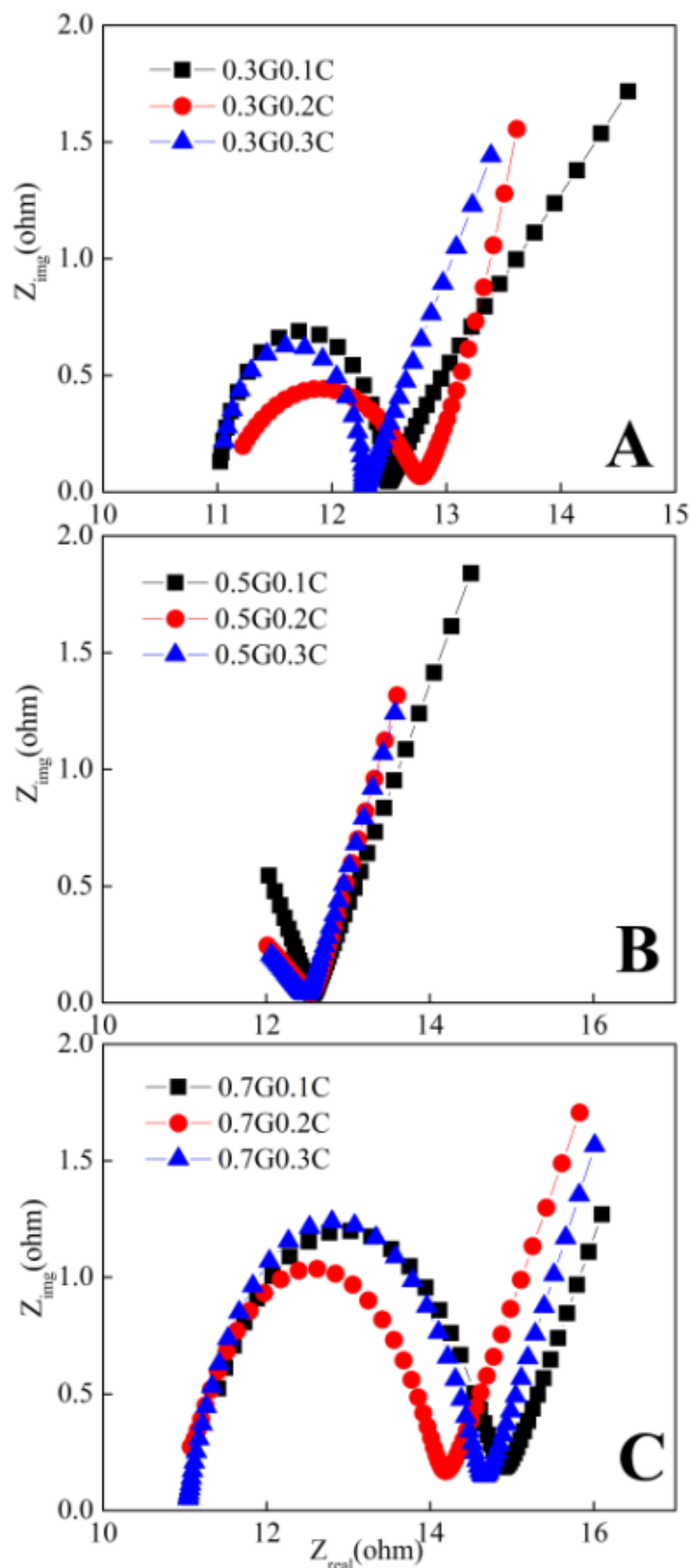
Figure S4 Nyquist plots of different AC air-cathodes at their OCPs. A: 0.3G*y*C, B: 0.5G*y*C, C: 0.7G*y*C.
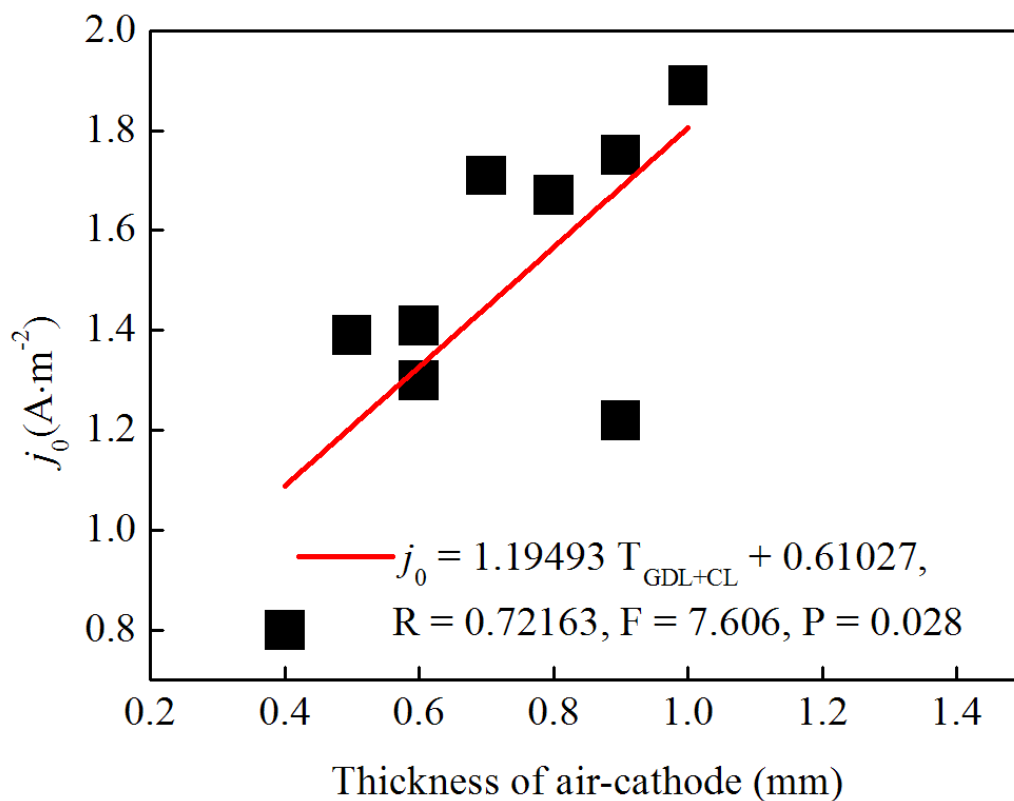
Figure S5 Linear fitting correlation between exchange current density (j_0) and the total thickness of air-cathode (T_{GDL+CL}).